Analysis strategy for multi-criteria optimization: Application to inter-seasonal solar heat storage for residential building needs

S. Launay, Benjamin Kadoch, O. Le Metayer, C. Parrado

▶ **To cite this version:**

S. Launay, Benjamin Kadoch, O. Le Metayer, C. Parrado. Analysis strategy for multi-criteria optimization: Application to inter-seasonal solar heat storage for residential building needs. Energy, 2019, 171, pp.419-434. 10.1016/j.energy.2018.12.181 . hal-02081049

HAL Id: hal-02081049
https://amu.hal.science/hal-02081049

Submitted on 27 Mar 2019

HAL is a multi-disciplinary open access archive for the deposit and dissemination of scientific research documents, whether they are published or not. The documents may come from teaching and research institutions in France or abroad, or from public or private research centers.

L'archive ouverte pluridisciplinaire **HAL**, est destinée au dépôt et à la diffusion de documents scientifiques de niveau recherche, publiés ou non, émanant des établissements d'enseignement et de recherche français ou étrangers, des laboratoires publics ou privés.

Energy 171 (2019) 419–434

Contents lists available at ScienceDirect

Energy

journal homepage: www.elsevier.com/locate/energy

Analysis strategy for multi-criteria optimization: Application to inter-seasonal solar heat storage for residential building needs

S. Launay [a], B. Kadoch [a, *], O. Le Métayer [a], C. Parrado [a, b, c]

[a] Aix-Marseille University, CNRS, IUSTI, Marseille, France
[b] Centro de Desarrollo Energetico Antofagasta (CDEA), Universidad de Antofagasta, Antofagasta, Chile
[c] Department of Civil Engineering, E.T.S. de Ingenieros de Caminos, Canales y Puertos, Universidad de Granada, Granada, Spain

ARTICLE INFO

Article history:
Received 7 September 2018
Received in revised form
21 December 2018
Accepted 24 December 2018
Available online 28 December 2018

Keywords:
Inter-seasonal thermal energy storage
Solar district heating
Multi-objective optimization
Sensitivity analysis
Renewable energy

ABSTRACT

As energetic systems become more and more complex, it is necessary to develop strategies for analyzing the influence of the parameters as well as their couplings. This approach is even unavoidable when the optimization procedure is based on multi-criteria. In the present work, we propose an analysis strategy for multi-criteria optimization applied to inter-seasonal solar heat storage for residential building energy needs, including heating and domestic hot water. The modeling is based on simplified equations of the components, while keeping the main physical and coupling phenomena. A sensitivity study is applied to the corresponding energetic system in order to identify the most relevant parameters and couplings interacting on the various output objectives. Several simulations are performed to investigate a multi-objective optimization and various figure representations are presented to refine the analysis.

© 2019 Elsevier Ltd. All rights reserved.

Nomenclature (main quantities)		
Quantities	Symbols	Units
Solar collectors surface	$S_{col} = S$	m^2
Inter-seasonal storage volume	$V_s = V$	m^3
Hot water tank volume	$V_{ws} = W$	m^3
Upper hot water tank volume	V_{wsu}	m^3
Bottom hot water tank volume	V_{wsb}	m^3
Inter-seasonal storage temperature	T_s	K
Solar collectors inlet temperature	T_{fe}	K
Solar collectors outlet temperature	T_{fs}	K
Difference between inlet and outlet temperatures of solar collectors	$\Delta T_{col} = D$	K
Upper hot water tank temperature	T_{wsu}	K
Bottom hot water tank temperature	T_{wsb}	K
Water network temperature	T_r	K
Solar fraction	F_s	
Solar collector efficiency	η	
Levelized cost of energy	$LCOE$	€/kWh

Indexes and Acronyms	
Quantities	Symbols
Solar heating system	SHS
Solar district heating	SDH
Domestic hot water	DHW

1. Introduction

Since the oil crisis of 1973, the energy flux management raised more and more interest in our society. This topic becomes even more attracting with the development of fluctuating renewable energies on the societal context of climate change. Among renewable energy sources, we can cite solar and wind energies that afford a technological and economic maturity. However, their energy production characteristics vary significantly in time, either at a hour, a day or a year. The variation and quality prediction of these characteristics depend on a given location and the surface of the concerned territory.

Precisely, the heat demand for space heating, whether for housing or tertiary activity, are in turn mostly seasonal in opposition to the solar resource. The realizations of the first projects with

* Corresponding author.
E-mail address: benjamin.kadoch@univ-amu.fr (B. Kadoch).

https://doi.org/10.1016/j.energy.2018.12.181
0360-5442/© 2019 Elsevier Ltd. All rights reserved.

the aim to accumulate solar heat in the summer to return it in winter have emerged from the 80's [1]. These projects were carried out both at the scale of a collective housing (building Toulouse in 1981) and at the neighborhood level (Sweden project in 1981 [1]). Major projects have been developed more specifically in the regions of Northern Europe. Although these regions are not particularly favorable toward a high density of solar energy, there are regions whose heat needs are large and where heating networks are already historically well developed. Adding to the district a solar collector field as a heat resource is not intended to fully cover the heating needs, but to substitute part of the fossil fuel or to cover additional energy requirements related to urban development. District heating and solar heating has got increased interest all over Europe in recent years and more than 100 plants with more than $500m^2$ of solar collectors have been put into operation since the mid 90's [2].

Monitoring the operation and performance of these facilities is useful to gather practical knowledge on specific cases. The collection of these data leads to guidelines for the design and sizing of future urban Solar District Heating (SDH) networks [3]. Because of the diversity of SDH, combining local characteristics relating among others to the resource and energy needs, the integration conditions for the solar collectors and the heat storage in the territory, there is no set of design rules. The works of [4] report some SDH of large scale systems connected to a borehole inter-seasonal storage. The ratio of the storage volume (V_s) on the solar collector area (Sc) of the demonstrators, Vs/Sc, is generally between 10 and 20 to provide a solar fraction F_s covering between 50 and 70% of the heating requirement. This ratio is in the range of 1–4 with a solar fraction between 35 and 70% of the needs for SDH installations connected to the water tank or gravel water inter-seasonal storage [5,6]. The study of [5] also combines the storage volume to the living area (A) heated by the SDH, with ratios Vs/A between 0.3 and 0.4 for some demonstrators in Germany. The Danish Energy agency, quoted by the paper [3], provides a first rough estimation of the optimal ratio between the storage volume and the solar collector area as function of solar fraction as $Vs/Sc \approx 5F_s - 1$.

Various studies of the literature validate their modeling work based on the data measured on the demonstrators [7–12]. The assumptions and modeled equations in these studies are not always clearly presented, and the control algorithm is rarely specified. The energy efficiency of the systems can combine the overall efficiency of the solar energy recovery with the solar fraction covering the heating needs. For [7], the overall efficiency of the plant is close to 30% for a solar fraction close to 100% of the heating requirements. In Refs. [7,8], the main energy losses are at the level of the solar collector and the heat storage, with equivalent efficiencies of around 55% each. In Refs. [9,10], the insulation performance is particularly studied for different configurations in climatically Turkey locations. The associated simulation results showed that the highest solar fraction is obtained for systems with storage buried into ground. The works of [11] showed that uncommonly large collector areas could increase the solar usability in North European existing houses resulting in around 50% solar contributions with small store sizes. In Ref. [12], a solar heating system designed to cover the annual load of a Switzerland housing area up to 95% has been optimized.

In fact, the overall system performance is due both to the intrinsic quality of the components, the relative size of these components involving more or less temperature variation during the annual operation cycle, and the characteristics and instructions for the SDH energy needs.

Performances of sensible heat inter-seasonal storage, either as water tanks [13], boreholes [14–16], near surface grounds [17,18] or aquifers [19], were analyzed by some heat transfer modeling approaches with more or less refinement. The influences of the storage parameters such as the type, the shape, the insulation quality, its implementation or integration under or out of the soil, the soil physical characteristics, have been particularly studied. For the storage of water tank type in Ref. [13], the management of the stratification phenomenon would improve the performance of the storage between 5 and 38 %. The layout, the design of deep boreholes, and their connection to optimize the energy flux management are highly dependent on the soil type as shown in Refs. [14,15]. In particular, the conter-flow heat exchange between the pipes has been studied in Ref. [16] with the help of a multipole method in order to predict axial temperature variations in boreholes. In Ref. [17], a literature review of ground-coupled heat pumps is presented and associated control is achieved. The works of [18] are aimed to investigate impact of surface boundary, climate and materials. In particular the authors found that system heat losses are strongly influenced by the performance of insulation layers. A detailed numerical simulation has been achieved in Ref. [19] to predict the performance of an aquifer thermal energy storage confined above and below by impermeable layers leading to good agreements with experiments.

In addition various energy and/or economic analyzes at the SDH scale are presented in the literature by setting and studying impacts of the collector area and the storage volume [9], the shape and type of the thermal storage [10,20] or the climate conditions [11]. In connection with the economic criteria, the results of these studies generally lead to an additional cost of energy produced compared to the use of conventional gas. The study presented in Ref. [10] exposes an investment payback of 19 years for the best scenario, and the works of [11] recommend limiting the solar fraction of about 40–50% for residential areas of Northern Europe for acceptable costs.

Multi-objective optimization on solar thermal systems has recently been applied by various authors [21–23]. The used optimization criteria include energy consumption, economic cost, environmental impact, and user dissatisfaction. The study is usually carried out on one or two criteria, which may be antagonistic. The works of [21] introduced a systematic approach to optimize simultaneously economic and environmental criteria for any climatic condition and heating demand profile. In Ref. [22], the multi-objective optimization technique corresponds to the genetic algorithm aimed to select the optimal solar thermal energy systems. The use of multi-objective optimization techniques presents all possible optimal solutions in the form of Pareto front in order to investigate the interaction of objectives. According to Ref. [23], the ultimate optimum values of the multi-objective functions on the Pareto front required a decision-making method with different weights for criteria, named as TOPSIS (Technique for Order Preference by Similarity to Ideal Solution). This method could be extended to three criteria [24,25] or more.

The quality of the optimization tools developed is due to the complementarity of the criteria taken into account and the parameters involved in the simulations. The relevance of the boundary conditions used in the calculations should also be added to these specifications. For [26], taking into account the time profiles for heating and Domestic Hot Water (DHW) is crucial in the sizing of energy systems. Without occupancy profile, the resulting demand profile does not show sharp peaks and no demand period, which is not realistic in a domestic house case. This raises questions about the choice of the modeling used in optimization: 1/a detailed modeling taking into account the physical characteristics of the energy system, including non-linear behaviors; 2/a modeling with a reduction of the complexities of the coupling mechanisms. The choice of the modeling will have a direct consequence on the

reliability of the result and the calculation time.

In this paper, we propose an analysis method to identify the dominant parameters affecting the robustness of SDH system performance. The SDH system under study includes two thermal storages, a long term and a short ones, to ensure heating and DHW needs respectively. The modeling is based on simplified equations of the components, while keeping the main physical and coupling phenomena. Particular attention is being conducted on the control and prioritization parameters of energy fluxes. The parametric study provides trends on the influence of parameters, but it is not always easy to quantify their respective sensitivity on the system behavior, especially when interactions between components can be significant.

2. Modeling description

The theoretical Hottel-Whillier equation is applied to design, develop and test flat-plate collectors in buildings [27]. The heating system is modeled in order to deliver a minimum temperature to the building, T_{demand}, therefore the apartment building itself was not analyzed in the assessment. The city of Marseille, in the south of France, is chosen. The environmental resources as solar irradiation and ambient temperature, among others were obtained from the meteo database of the TRNSYS software. The study is particularly focused upon the regulation and optimization of some crucial variables such as: the volume of the inter-seasonal storage tank V_s, the surface of solar collectors S_{col}, the difference of temperature between the inlet and the outlet of the solar collectors ΔT_{col} , the volume of the hot water tank V_{ws}.

A schematized view of the whole system is represented in Fig. 1. In the following subsections the description of physical models is presented for each component.

2.1. Solar collector

The solar collector receives a global flux (direct and diffuse fluxes) from the sun and produces heat as output. The heat is transported by the heat transfer fluid (HTF), from the inlet to the outlet of the collector. Not all the irradiation is converted in useful heat, due to heating losses, optic efficiency of the glass and different weather condition depending on the location [27]. According to Ref. [27], the useful heat Q_u can be expressed as follows,

$$Q_u = S_{col} F_r \left(\varphi_{sa} - K_{amb} \left(T_{fe} - T_{amb} \right) \right) \tag{1}$$

where S_{col}, F_r, T_{fe} and T_{amb} correspond respectively to the surface of the solar collectors, the collectors heat removal factor, the inlet fluid temperature in the solar collectors and the ambient temperature. φ_{sa} corresponds to the absorbed solar flux calculated according to the various selective optic efficiency of the glass and the absorber, as well as the orientation and angle of the solar collectors. In this relation K_{amb} represents the global heat transfer coefficient between the absorber plate and the ambient from the front and back plates of the solar collectors (including convective, radiative and conduction heat transfers).The collector heat removal factor F_r, which takes into account the non-uniform temperature distribution along the solar collectors field, can be expressed as follows [28],

$$F_r = \frac{\dot{m}_{rsn} c_w}{S_{col} K_{amb}} \left(1 - exp\left(- \frac{S_{col} F' K_{amb}}{\dot{m}_{rsn} c_w} \right) \right) \tag{2}$$

where $\dot{m}_{rsn}$, c_w and F' correspond respectively to the mass flow rate, the specific heat capacity of the fluid and the modified efficiency factor of the collectors.The useful heat Q_u can also be defined by the energy balance equation,

$$Q_u = \dot{m}_{rsn} c_w \left(T_{fs} - T_{fe} \right) \tag{3}$$

where T_{fs} is the outlet fluid temperature of the solar collectors. In order to decrease the quantity of equation for the computational

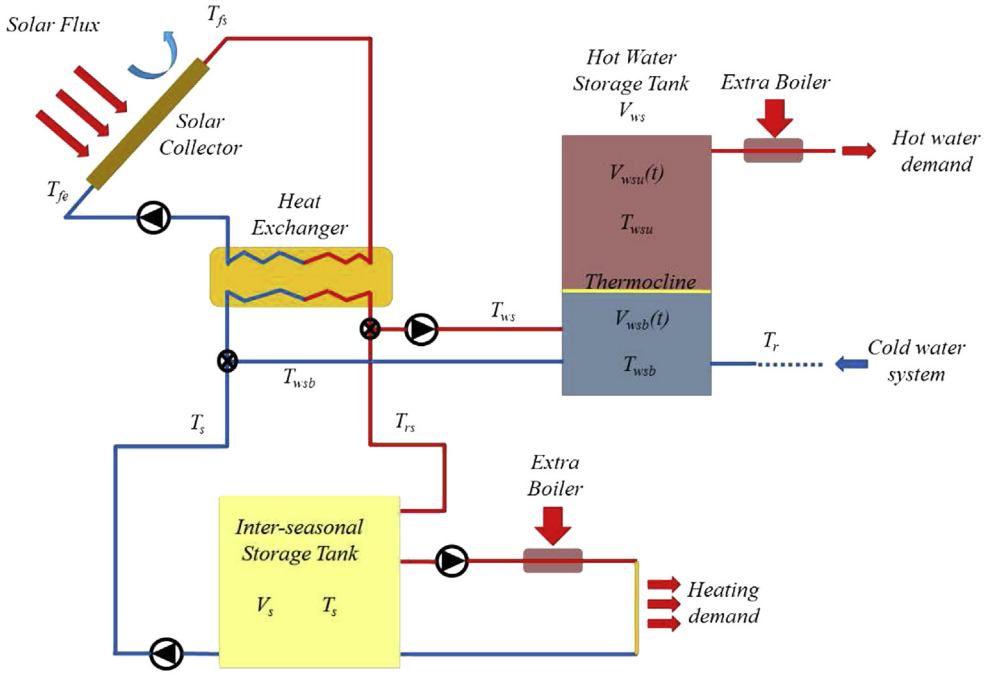

Fig. 1. Scheme of the solar heating system with seasonal sensible heat thermal storage (SHS-SSHTS) and hot water storage.

model, the three preceding equations are mixed as follows,

$$\Delta T_{col} = \left(T_{stag} - T_{fe}\right)\left(1 - exp\left(-\frac{S_{col}F'K_{amb}}{\dot{m}_{rsn}c_w}\right)\right) \quad (4)$$

where $T_{stag} = T_{amb} + \frac{\varphi_{sa}}{K_{amb}}$ is the stagnation temperature depending on meteorological conditions and,

$$\Delta T_{col} = T_{fs} - T_{fe} \quad (5)$$

The only unknowns appearing in relation (4) are: T_{fe}, T_{fs} and $\dot{m}_{rsn}$. Other values are either constant parameters or known inputs. The solar collectors orientation and inclination are also taken into account following [29].

2.2. Heat exchanger

A single heat exchanger is used to perform sensible heat storage either in the inter-seasonal storage (ISS) or in the hot water storage (HWS) alternately. The contribution of the heat exchanger is modeled as the efficiency of the exchanger between the heat produced by the solar collector (SC) and the heat stored by the inter-seasonal storage (ISS) or the hot water storage (HWS). The equation can be expressed by,

$$E_{SC} = \frac{\dot{m}_{rsn}c_w\left(T_{fs} - T_{fe}\right)}{\dot{m}_{rsn}c_w\left(T_{fs} - T_{min}\right)} \quad (6)$$

where T_{min} corresponds to the outlet temperature of one of the heat storage based on regulation conditions. Thus the value of T_{min} corresponds to the temperature of the inter-seasonal storage tank or the outlet temperature from the hot water storage tank denoted respectively by T_s and T_{wsb}.After simplifications and use of relation (5), the efficiency E_{SC} of the exchanger can be computed as follows,

$$E_{SC} = \frac{\left(T_{fs} - T_{fe}\right)}{\left(T_{fs} - T_{min}\right)} = \frac{\Delta T_{col}}{\left(T_{fs} - T_{min}\right)} \quad (7)$$

In addition the thermal balance applied to the heat exchanger leads to the following relation,

$$\dot{m}_{rsn}c_w\left(T_{fs} - T_{fe}\right) = \dot{m}_{rsn}c_w(T_{max} - T_{min}) \quad (8)$$

where T_{max} corresponds to the inlet temperature of one of the heat storage. The value of T_{max} corresponds to the inlet temperature of the inter-seasonal storage tank or the hot water storage tank denoted respectively by T_{rs} and T_{ws}.The relation (8) rewrites,

$$\Delta T_{col} = T_{fs} - T_{fe} = T_{max} - T_{min} \quad (9)$$

The unknowns appearing in relations (7) and (9) are: T_{fe}, T_{fs}, T_{min} and T_{max}.

2.3. Inter-seasonal storage tank

In Europe, around half of the total heating requirement of a domestic building occurs during mid-winter when the solar radiation is not able to meet the demand itself [30]. Due to the scarcity of solar radiation during almost two months of the year, several solutions to store the energy produced in summer as inter-seasonal thermal storage were proposed [13]. In this study a cylindrical metal tank located inside the ground is used and filled with water at an homogeneous temperature T_s.

The temporal evolution of the storage temperature T_s obeys the following equation,

$$\rho_w c_w V_s \frac{dT_s}{dt} = \phi_{ent\_rs} - \left(\phi_{dem} - \phi_{supply}\right) - \dot{Q}_{losses} \quad (10)$$

where ρ_w and V_s correspond respectively to the liquid density and the volume of the tank. The water is chosen as the storage material, due to its high specific heat capacity c_w and its good performance in sensible storage systems [31]. In relation (10), ϕ_{ent_rs} is the heat energy provided by the solar collector and stored in the inter-seasonal solar tank. This one is computed as follows,

$$\phi_{ent\_rs} = \dot{m}_{rsn}c_w(T_{rs} - T_s) \quad (11)$$

In relation (10), ϕ_{dem} corresponds to the power necessary to supply the heating demand of the building and reads,

$$\phi_{dem} = U_{bu}S_{bu}\left(T_{comfort} - \overline{T}_{amb}\right) - \phi_{sources} \quad (12)$$

where $U_{bu}S_{bu}$ corresponds to the global thermal conductance of the building. $T_{comfort}$ is the desired comfort temperature inside the building and $\overline{T}_{amb}$ is the outside mean temperature of the previous 24 h. Using $\overline{T}_{amb}$ instead of instantaneous outside temperature is a simple way to integrate the building thermal inertia whose quantity depends on time integration [29]. Finally $\phi_{sources}$ corresponds to internal heat sources such as direct solar gain or human activities. The study of the variability of internal sources is not the subject of this paper and $\phi_{sources}$ is thus considered as a constant.In relation (10), ϕ_{supply} is the power (from a boiler) that needs to be added to the solar contribution in order to complement the heating demand of the building. This extra power can be computed as,

$$\phi_{supply} = \phi_{dem} - \phi_{stor\_av} - \phi_{ent\_rs} \quad (13)$$

where ϕ_{stor_av} corresponds to the stored available heat inside the tank,

$$\phi_{stor\_av} = \rho_w c_w V_s \frac{d(T_s - T_{demand})}{dt} \quad (14)$$

In relation (10), T_{demand} corresponds to the set-point temperature of the heating, which is sensitive to the heating mode of the building (heating floor, radiator, etc.). $\dot{Q}_{losses}$ corresponds to the thermal losses associated to the inter-seasonal storage tank,

$$\dot{Q}_{losses} = h_t S_t (T_s - T_g) \quad (15)$$

where h_t, S_t and T_g are respectively the global heat transfer coefficient between the tank and the ground, the surface of the tank and the ground temperature. The associated insulation corresponds to glass wool which thermal conductivity is $0.03W/(m.K)$ and its thickness is $0.4m$.The only unknowns appearing in relation (10) are: T_s, T_{rs} and $\dot{m}_{rsn}$. Other values are either constant parameters or known inputs.

2.4. Hot water tank

In this study a cylindrical hot water tank is considered for hot water needs. The thermal-hydraulic behavior of the hot water storage tank is assumed to be stratified type. Then this tank is divided into 2 sub-volumes separated by a thermocline. The hot water tank model presented in this section has been

experimentally validated in Ref. [32]. The temperature of upper and lower parts are denoted respectively by T_{wsu} and T_{wsb}. The temperature of the upper part is assumed to be constant corresponding to the needed hot water demand. The lower storage tank temperature T_{wsb} is assumed to be uniform because of fluid mixing process caused by simultaneous solar heat charging and DHW draw off. The time evolution of the lower storage tank temperature T_{wsb} obeys the following equation,

$$\rho_w c_w V_{wsb}(t) \frac{dT_{wsb}}{dt} = \phi_{ent\_ws} - \dot{m}_{rsw} c_w (T_{wsb} - T_r) \tag{16}$$

where $V_{wsb}(t)$ corresponds to the lower sub-volume of the tank depending on time, $\dot{m}_{rsw}$ and T_r correspond respectively to the liquid mass flow rate according to the hot water demand ϕ_{ent_dem} and the temperature of the inner cold water (from the water network).In relation (16) ϕ_{ent_ws} is the heat provided by the solar collector and stored in the hot water tank. It is computed as follows,

$$\phi_{ent\_ws} = \dot{m}_{rsn} c_w (T_{ws} - T_{wsb}) \tag{17}$$

where T_{ws} is the inlet temperature of the lower sub-volume water tank.ϕ_{ent_dem} corresponds to the heat flux necessary to supply hot water needs and reads,

$$\phi_{ent\_dem} = \dot{m}_{rsw} c_w (T_{wsu} - T_r) \tag{18}$$

The relation (16) is supplemented by the following evolution equation of the sub-volume,

$$\rho_w \frac{dV_{wsb}}{dt} = \dot{m}_{rsw} \tag{19}$$

When the hot water tank energy is not sufficient enough to preserve the whole demand an extra boiler is taken into account to complement this one and reads as follows,

$$\phi_{w_{supply}} = \dot{m}_{rsw} c_w (T_{dem} - T_{wsb}) \tag{20}$$

This boiler consists in heating the water from the tank to get the expected set-point temperature of DHW $T_{dem} = T_{wsu}$. The only unknowns appearing in relations (16–20) are: T_{wsb}, T_{ws} and $\dot{m}_{rsn}$. Other values are either constant parameters or known inputs.

2.5. Regulation conditions and associated parameters

Regulations concerning fluid circulation need to be added to the preceding computational models. According to the focusing of this study, the heat is stored as sensible heat. Thus the temperature of the storage T_s cannot be higher than $373.15K$. If this one reaches a value close to the boiling temperature then the mass flow rate $\dot{m}_{rsn}$ will be equal to zero and the fluid circulation among the solar collector is stopped.

It was also defined a minimum value for the mass flow rate $\dot{m}_{rsn}$: $\dot{m}_{rsn\_min}$. If $\dot{m}_{rsn}$ has values lower than $\dot{m}_{rsn\_min}$, then fluid circulation is stopped and $\dot{m}_{rsn}$ is set to zero.

Another regulation is linked to the temperature of stagnation T_{stag} defined in the solar collector device. Fluid circulation is allowed if the difference between T_{stag} and T_s, or alternately T_{sw}, is higher than a fixed value ΔT_{on}. The fixed value ΔT_{on} corresponds to the minimum temperature difference in order to limit the cycles of on/off circulation in the solar collector.

Priority has been chosen to perform the hot water tank filling when dealing with solar energy. Then the heating storage circulation is only enabled when the energy available in the hot water tank is at maximum ($T_{dem} = T_{wsb}$). The hot water tank circulation from the solar collector exchanger is enabled when the sub-volume V_{wsb} becomes higher than a fixed value V_{lim} considered as a parameter in this work.

At least for the current study, a constant value of 0.8 is set for the exchanger efficiency E_{SC} corresponding to a common value for heat plate exchangers.

2.6. Output objective criteria

In order to quantify the performance of the inter-seasonal solar system simulated in the present study, three objective criteria are selected. The two first ones are deduced from the energy analysis while the third one is dedicated to economic analysis.

The first output criterion is the “solar fraction” F_s. It corresponds to the part of the solar thermal energy in the thermal energy used to ensure DHW and the building thermal comfort. The solar fraction is based on the supply energy and the useful energy calculated over the year and reads:

$$F_s = 1 - \frac{E_{Supply\ energy}}{E_{Heating} + E_{DHW}} \tag{21}$$

The second criterion is the “solar collector efficiency” η. It corresponds to the thermal solar productivity (kWh/m^2 of solar collector) divided by the solar irradiation, which are calculated step by step and integrated all over the year:

$$\eta = \frac{E_{thermal\ solar\ collector}}{E_{solar\ irradiation} \cdot S_{thermal\ collector}} \tag{22}$$

The third criterion is the “Levelized cost of energy” *LCOE*. It corresponds to the sum of all the cost incurred during the lifetime of the project divided by the units of the total heat energy demand during the same period. The criterion is given by:

$$LCOE(€/kWh) = \frac{Total\ Cost}{N_{year} \cdot (E_{Annual_{Heat}} + E_{Annual_{DHW}})} \tag{23}$$

where N_{year} is the project lifetime. The total cost is calculated as:

$$Cost = Cost_{investment} + Cost_{maintenance} + Cost_{operation} \tag{24}$$

The investment cost in the inter-seasonal storage is based on data collected in the literature ([6,33]). It should be noted that, at the difference of the energy criteria (F_s and η), the economic criterion may be largely dependent on the market price evolution, which is sensitive to the industry investment for more intensive production in this kind of energy system.

3. Results

The time-dependent preceding model is simulated using the software Open Modelica [34]. Open Modelica is an open source Modelica-based modeling and simulation environment used in industrial and academic fields. The time step corresponds to 10 min and available meteorologic data are linearly interpolated. This corresponding time step corresponds to the characteristic time scale of the hot water tank demand. Simulations with either lower time steps or cubic weather data interpolation showed no more significant changes on results.

In order to get global energy results not dependent of the initial conditions, specifically for the inter-seasonal storage conditions, the analysis focused on the fourth year of the simulation, which

Table 1
Main parameters for the reference case.

V_s	S_{col}	ΔT_{col}	V_{ws}	V_{lim}	ΔT_{on}	T_r	T_{wsu}	$T_{comfort}$	T_{demand}
m^3	m^2	K	m^3	m^3	K	$°C$	$°C$	$°C$	$°C$
200	120	7	1.2	0.4	5	15	60	20	30

shows no significant annual energy efficiency difference when compared to the third year.

In the following subsections the dynamical results for the reference case, sensitivity analysis and optimization will be presented.

3.1. Reference case of study

Table 1 summarizes the values of the parameters used for the reference case. The modeled system is a building of 8 houses, inspired of one Switzerland building realization [35], but located in the city of Marseille. The surface of solar collectors S_{col} has been reduced to stay with similar solar resource as Swiss case. The value of the internal heat sources $\phi_{sources}$ is assumed to be constant: $200W$. The solar collectors are oriented south with an inclination of $55°$. The dwelling follows the standard of the French RT 2012 of low-energy buildings, *i.e.*, the energy needs for heating, air conditioning and DHW must not exceed $50kWh/(m^2.year)$. The heating temperature T_{demand} is set to $30°C$, adapted to floor heating conditions, and the DHW is set to $60°C$ at the DHW tank outlet in order to respect the sanitary regulation. The DHW storage volume $V_{ws} = 1.2m^3$ corresponds to the daily DHW consumption of the building. T_r and $T_{comfort}$ corresponds respectively to the water network and building comfort temperatures.

For the annual balance, the total energy needs are equal to $43MWh$ for building heating and to $20MWh$ for DHW, which corresponds to $\sim 43kWh/(m^2.year)$. Based on meteo data of the city of Marseille and with an inclination of $55°$ of the solar collector oriented South, $64MWh$ are collected from the solar thermal panels along the year. 11% of the collected solar thermal energy is used to cover the inter-seasonal storage heat losses. In order to cover the global thermal energy needs, $5MWh$ ($4MWh$ for heating and $1MWh$ for DHW) of supply energy (gas, petrol, or electricity) are necessary. For the reference case, based on a lifetime project of 30 years, "solar fraction", "levelized cost of energy" are equals to 0.91, $0.095 €/kWh$, respectively. The yearly efficiency of the solar thermal collectors ("collector efficiency") is equal to 0.39 with a mean operation time

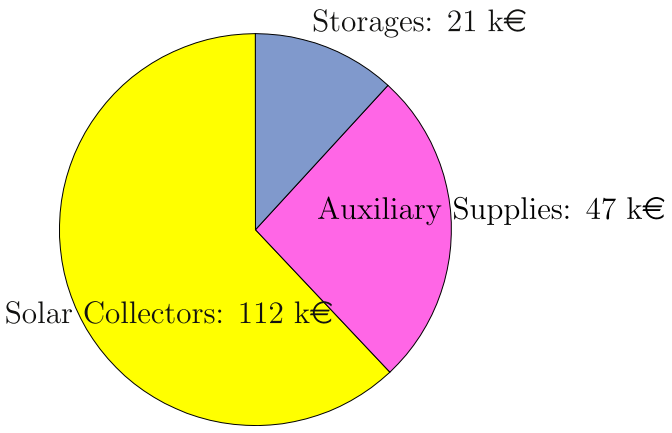

Fig. 2. Global costs of the principal system components.

corresponding to 59% of the day. The investment, maintenance and operation costs during the lifetime are 83, 48 and 48 $k€$, respectively. Global costs of the principal system components, in Fig. 2, shows that solar collector, the supply energy components and the storages are responsible for 62%, 26% and 12% of the total cost, respectively.

Fig. 3 (top) shows the monthly dynamics of the system considered over a full year. Heating needs are not insured by the inter-seasonal heat storage mainly in February. It is noted that from February to September, the system is able to constitute the energy storage, and the storage heat is gradually used during the season of fall and the beginning of winter. The solar energy recovery is not optimal in summer because the energy level in the inter-seasonal storage is at its maximum level from July to October. During this period, the solar collector main operation is used for daily DHW needs and to cover thermal losses of the inter-seasonal storage. Fig. 3 (bottom) shows the results obtained for an inclination of $35°$ of the solar collector. The results behavior is very similar as for $55°$ inclination. Heating needs are also not insured in February and the use of supply energy is much more pronounced in January for an inclination of $35°$. The system is also able to constitute the energy storage from February to September. The differences are explained by a better valuation of solar energy during winter and a worse valuation during summer in the $55°$ inclination case. This confirms the choice of $55°$ inclination of solar collectors in Marseille since the heating needs appears mainly during winter.

Auxiliary heat energy for DHW production may happen at different days all along the year. It happens when solar irradiation resource is very low during several consecutive days and which takes place the most often at mid-season at Marseille. Fig. 4 (top) shows the energy needs and consumptions, and the state of the DHW tank during five consecutive days in the month of February (11–16 th) and May (15–20 th). For this scenario, the DHW profile is similar for both periods with three peaks each days, corresponding to the morning, noon and the evening. In Fig. 4 (bottom), it corresponds to the non-dimensional temperature and volume of the water in the lower part of the DHW tank, below the thermocline (eq. (16) and eq. (19)). When V_{wsb}/V_{ws} is equal to one, that means the thermocline is at the top of the tank. In consequence for February, the DHW at $60°C$ is no more available and extra energy is consumed to insure DHW demand. As $(T_{wsb} - T_r)/(T_{wsu} - T_r)$ reaches the value of one, that means the DHW tank is completely charged at $60°C$ due to solar energy contribution. The position of the thermocline is then reset at level 0 (bottom of the DHW tank). As we can see for February case, the solar energy contribution is not sufficient to entirely complete the DHW tank to the set point temperature. Auxiliary heat energy is then consumed. Similar results are presented in Fig. 4 (right) for a period of May. As the solar energy resource is quite high according to DHW demand, the DHW tank is refilled every day with repetitive behavior for these boundary conditions.

3.2. Sensitivity analysis

A sensitivity study is carried out to quantify the influence of parameters and their interactions on a model response [36,37]. The sensitivity analysis used is based on a 2^N factorial plan of experiments [38], where N is the number of parameters x_i. Each parameter takes two levels (minimum & maximum values) chosen from a reference value ($mean(x_i) = x_{ref}$). This method enables to quantify the influence of the different parameters and their interactions for a given output objective y. The main principle is to approximate the system response as function of normalized input parameters or factors X_i:

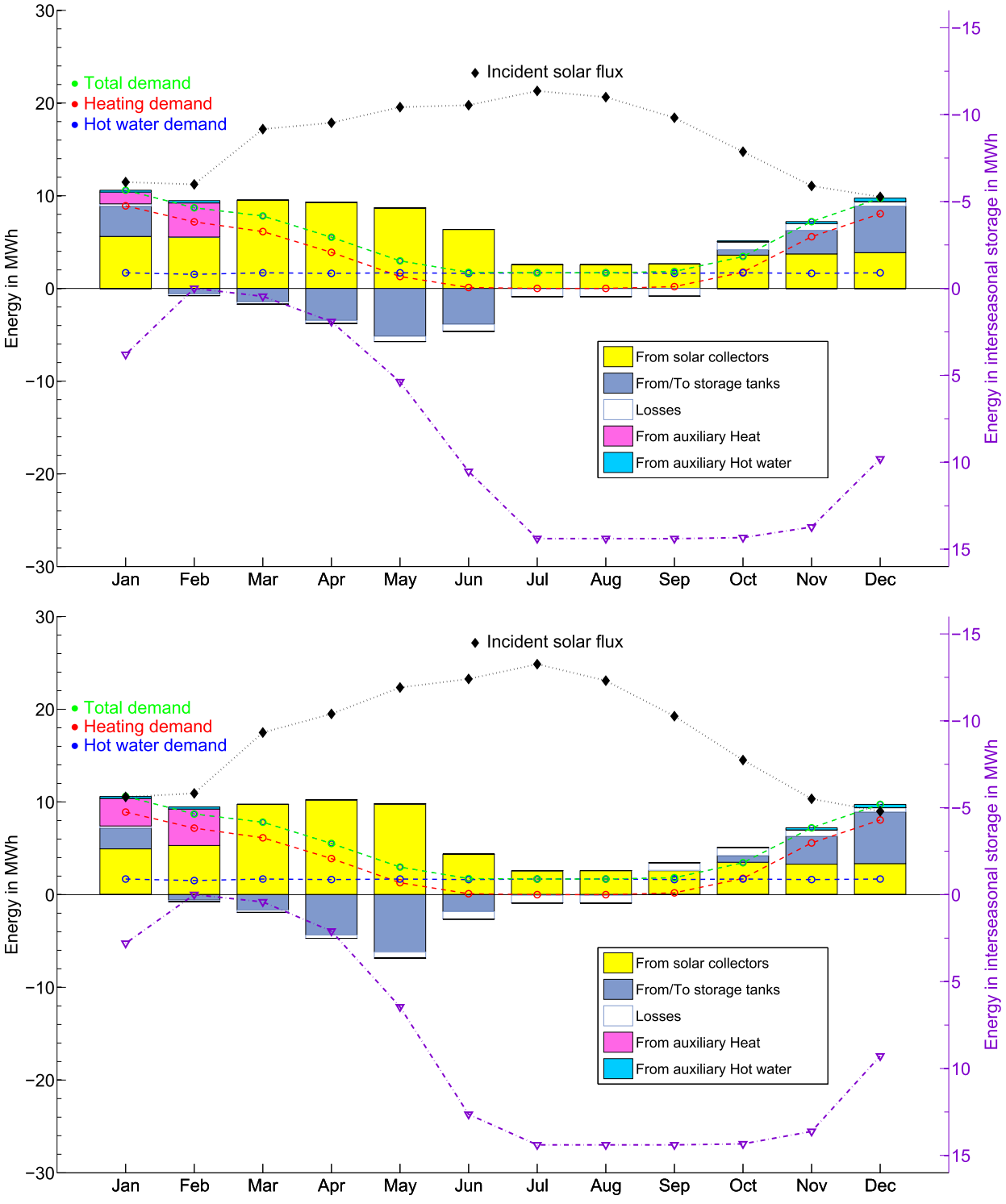

Fig. 3. Reference case: monthly dynamics of energy needs and demands over a year. The inclination of the solar collector are 55° (top) and 35° (bottom).

$$y = \beta_0 + \sum_{i_1=1}^{N} \beta_{i_1} X_{i_1} + \sum_{i_1=1}^{N} \sum_{i_2>i_1}^{N} \beta_{i_1 i_2} X_{i_1} X_{i_2} + \sum_{i_1=1}^{N} \sum_{i_1>i_2}^{N} \sum_{i_3>i_2}^{N} \beta_{i_1 i_2 i_3} X_{i_1} X_{i_2} X_{i_3} + \ldots + \beta_{i_1 i_2 \ldots i_N} X_{i_1} X_{i_2} \ldots X_{i_N} \quad (25)$$

$$X_i = \frac{x_i - x_{i_{ref}}}{(max(x_i) - min(x_i))/2}, \mathrm{i} = 1, \mathrm{N} \quad (26)$$

where the subscript $_{ref}$ denotes the reference case. By solving the linear system described in eq. (25), we obtain the different effects $\beta = \beta_0, \beta_{i_1}, \beta_{i_1 i_2}, \ldots, \beta_{i_1 i_2 \ldots i_N}$. We can note that β_0 corresponds to the mean of the output objective y calculated for all parameter sets.

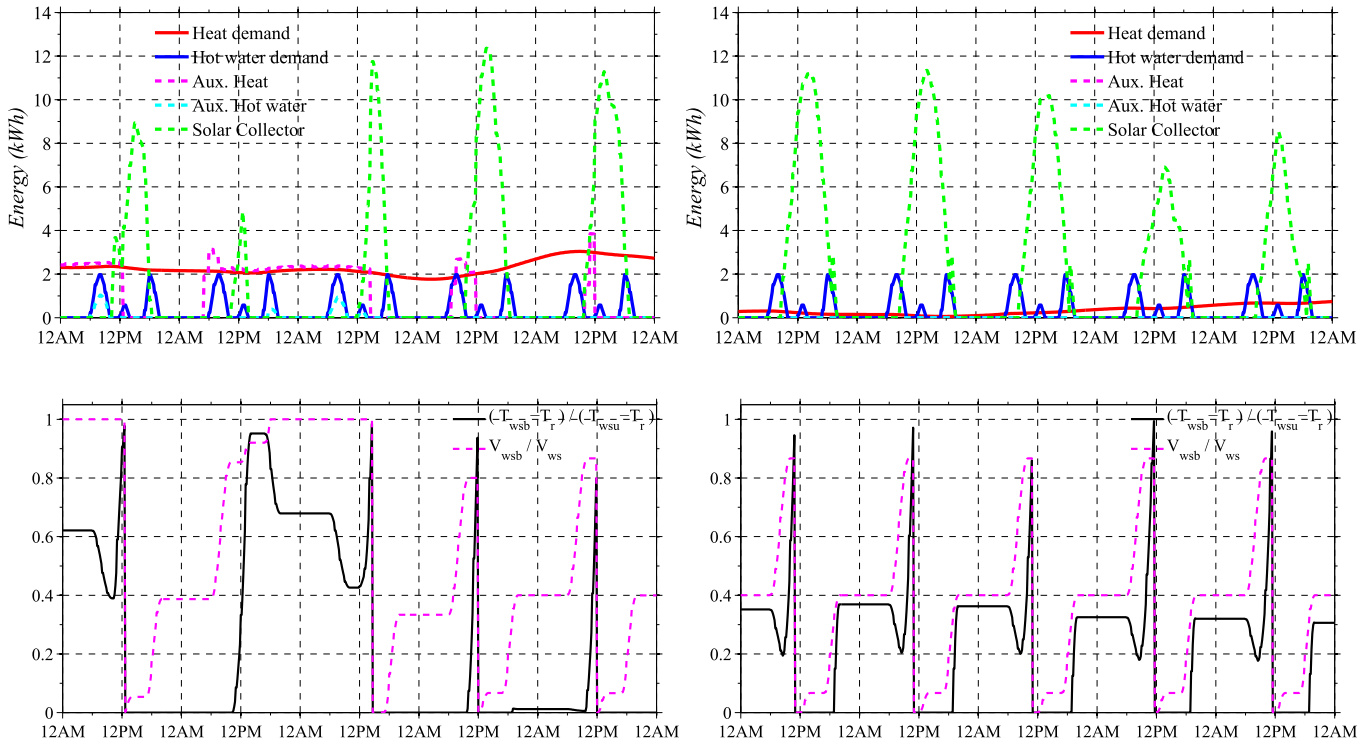

Fig. 4. Energy levels for demands and resources (top) and time evolution of temperature and volume of cold water in DHW storage (bottom) for 5 consecutive days in February (left) and May (right). 12*AM* and 12*PM* refers to midnight and midday, respectively.

Table 2
Parameter levels for the sensitivity study with $N = 5$ parameters.

x_i	Reference	Variation	min	max
$V = V_s(m^3)$	200	±50%	100	300
$S = S_{col}(m^2)$	120	±30%	84	156
$D = \Delta T_{col}(K)$	7	±42.9%	4	10
$W = V_{ws}(m^3)$	1.20	±50%	0.60	1.80
$L = V_{lim}/V_{ws}(\%)$	1/3	±25%	0.25	0.42

We also introduce the sum of squares *SS* for different effects, which measures the percentage contribution of each model term relative to the total sum of squares *SST*.

$$SS_i = 2^N \beta_i^2, i = 1, 2^N - 1 \tag{27}$$

$$SST = \sum_{i=1}^{2^N-1} SS_i = \sum_{i=1}^{2^N} y_i^2 - \frac{\left(\sum_{i=1}^{2^N} y_i\right)^2}{2^N} \tag{28}$$

where $y_i, i = 1, 2^N$ are the different output quantities from 2^N simulations.

In our study, $N = 5$ input parameters of the model are considered: $V = V_s$, $S = S_{col}$, $D = \Delta T_{capt}$, $W = V_{ws}$ and $L = V_{lim}/V_{ws}$. Table 2 summarizes the levels for the parameters considered by the

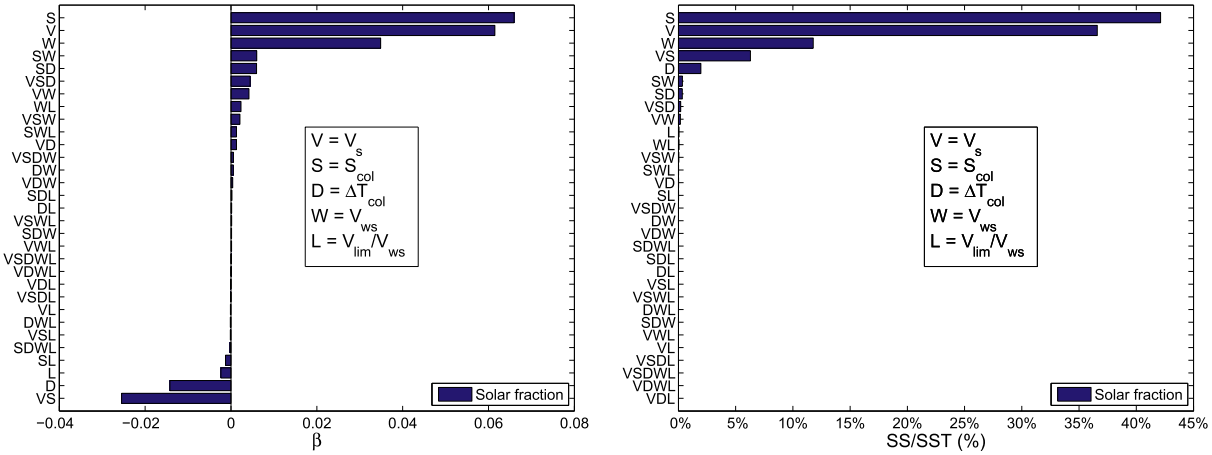

Fig. 5. Sensitivity on solar fraction: β coefficients (left) and normalized sum of squares *SS*/*SST* (right).

sensitivity study.

3.2.1. Solar fraction objective

Fig. 5 illustrates the sensitivity of "solar fraction" to parameters and combined parameters. The sense and the variability of the different effects and of their interactions are shown in Fig. 5 (left) and in Fig. 5 (right), respectively. The surface of the solar collectors S_{col} and the volume of the inter-seasonal storage tank V_s dominate the process accounting for $\sim 42\%$ and $\sim 37\%$ of the total variability, respectively. Both effects are positive, this suggests so that increasing S_{col} and V_s from their low levels to their high levels will increase the "solar fraction". This result is expected since increasing the volume of the inter-seasonal storage tank or the surface of the solar collectors will enhance more the capture of solar energy or its storage. The effect due to the volume of DWH V_{ws} still be significant with $\sim 12\%$ and it is also positive. The interaction effect V_sS_{col} ($\sim 7\%$) is also important for the system. However the effect of V_sS_{col} (Fig. 5 (left)) is negative. This means that, comparing to the first orders (S_{col} and V_s), the combination of these effects are attenuated by their interaction. Finally, the regulation parameter ΔT_{col}, which corresponds to the temperature difference between the solar collector inlet and outlet used in the mass flow rate regulation, has a very weak negative effect ($\sim 2\%$) for the sizing of the present study. The other factors and their interactions do not show strong variations for the "solar fraction".

3.2.2. Levelized cost of energy objective

Fig. 6 shows the sensitivity of the objective *LCOE* which should be minimized. The surface of the solar collectors S_{col} is responsible for the major part of *LCOE* accounting for $\sim 51\%$ of the total variability and its effect is positive. Indeed, increasing the surface of the solar collectors will not value significantly the solar energy and will not involve thus a large decrease of the auxiliary energies, in comparison with the additional costs. This shows that S_{col} is oversize concerning this system. The effects due to V_{ws} ($\sim 18\%$), V_s ($\sim 16\%$) and the interaction effect V_sS_{col} ($\sim 10\%$) are of lesser importance but has to be taking into account. The effects of V_{ws} and V_s are negative since the gain due to a better energy storage

Table 3
Best configuration for the three main objectives.

Objective	V_s	S_{col}	ΔT_{col}	V_{ws}	V_{lim}/V_{ws}
	m^3	m^2	K	m^3	%
Max: solar fraction	200	156	4	1.8	0.25
Min: *LCOE*	300	91.2	4	1.8	0.42
Max: collector efficiency	300	84	4	1.56	0.25

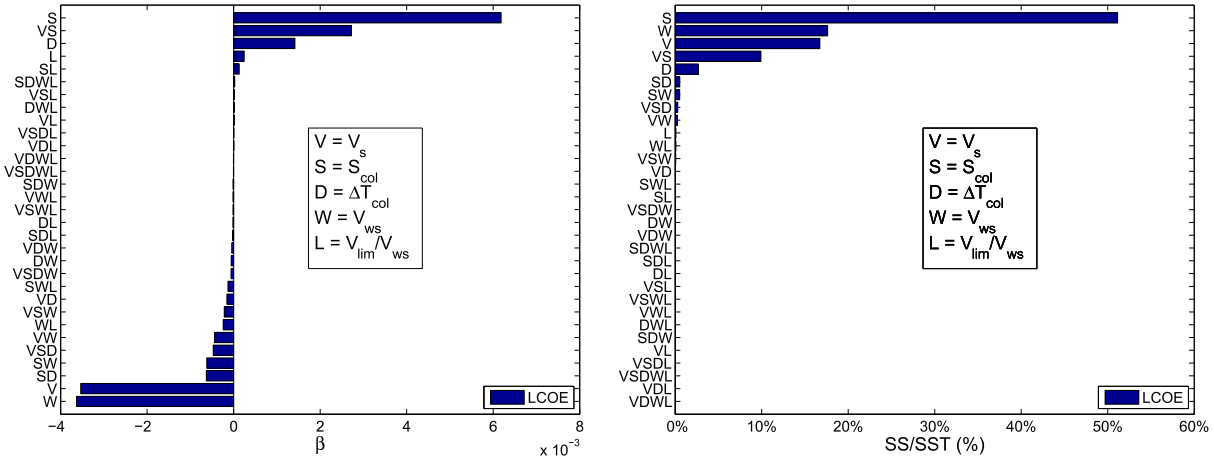

Fig. 6. Sensitivity on levelized cost of energy: β coefficients in $€/kWh$ (left) and normalized sum of squares SS/SST (right).

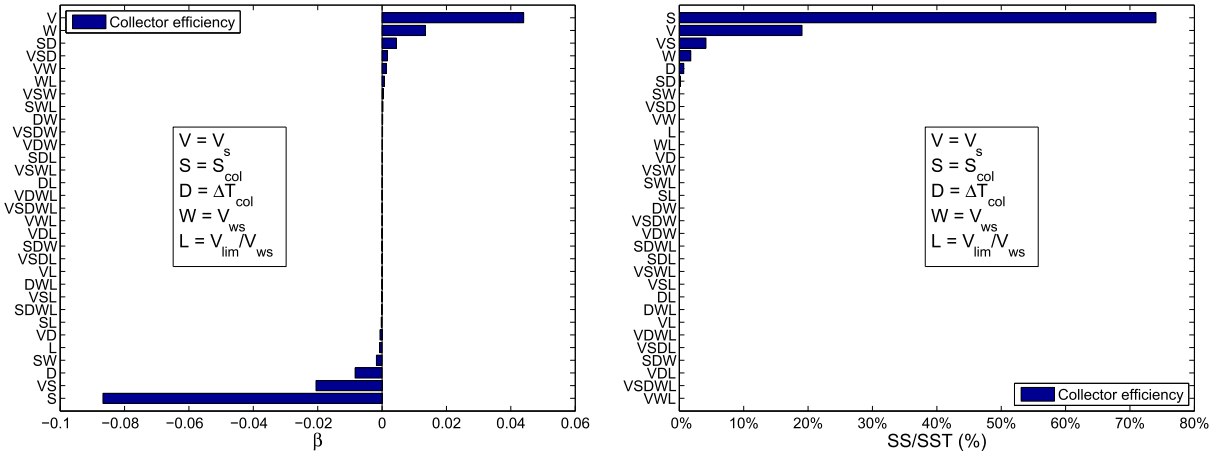

Fig. 7. Sensitivity on collector efficiency: β coefficients (left) and normalized sum of squares SS/SST (right).

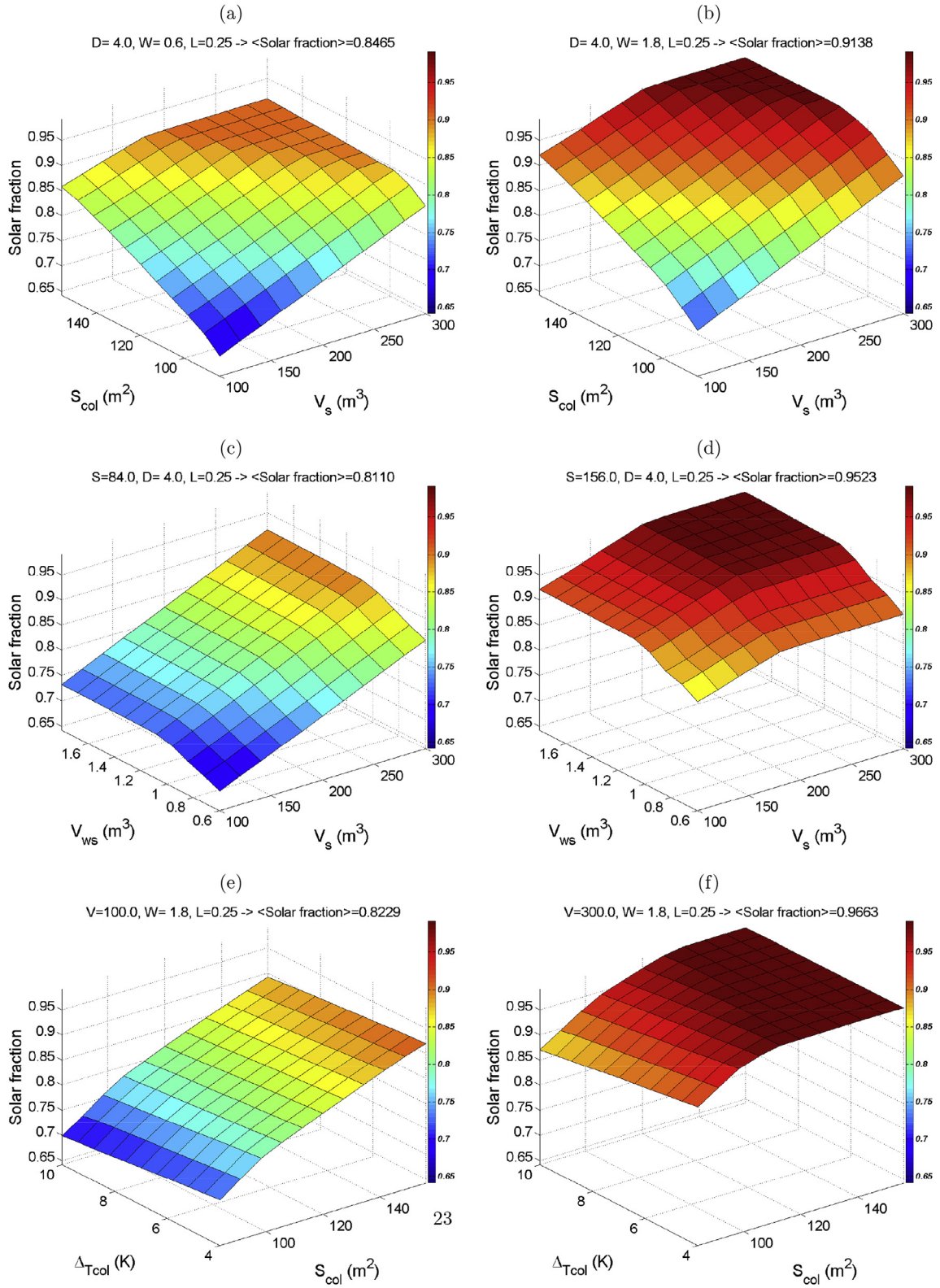

Fig. 8. Solar fraction as function of the different parameters. The information given on the top of each plots corresponds to the values of the parameters keeping constant and to the ensemble average $\langle \bullet \rangle$ of the criterion for the corresponding plot.

compensate largely the extra costs for larger size of storage. At the opposite, the effect of S_{col} is positive which means that the additional energy received for a larger surface of collectors does not bring significant gain in comparison of the additional costs generated. The interaction effect $V_s S_{col}$ will accentuate the economic loss obtained by increasing S_{col} and attenuate the gain by increasing V_s. The other effects can be considered as negligible.

3.2.3. Collector efficiency objective

The sensitivity of "collector efficiency" are plotted in Fig. 7. Its behavior is almost the opposite of the one of *LCOE*. Indeed, the same explanations as *LCOE* can be applied for "collector efficiency". The surface of the solar collectors S_{col} is also responsible for the major part accounting for $\sim 74\%$ of the total variability with a positive effect. The notable differences concern the effect of V_s which is a little more important with $\sim 19\%$ and the effect of V_{ws} ($\sim 2\%$) which is negligible. The difference with *LCOE* is due to the fact that the investment and the maintenance are taken into account in this objective. Consequently, the "collector efficiency" gain due to V_{ws} is negligible in front of one due to V_s while the extra-cost for increasing V_s becomes less and less important. In other words, the study of "collector efficiency" gives trend information to what would be obtained for the *LCOE*: maximize the effectiveness of the collector's should tend to minimize the *LCOE*. The latter assertion is only true as long as the cost of make-up energy is cheaper than solar energy.

3.3. Optimization

In order to investigate multi-objective optimization, several simulations are performed by using a regular discretization of the $N = 5$ parameters retained for sensitivity study (Table 2). Each parameter vary thus from its minimum value to its maximum value using $N_p = 11$ points. $N_p^N = 161051$ simulations are therefore carried out. Table 3 shows the values of the parameters to be chosen for the different objective criteria. ΔT_{col} has to be minimum for every objectives and V_{ws} maximum for "solar fraction" and *LCOE*. S_{col} is maximum for "solar fraction" and minimum for the two another and V_s is maximum for *LCOE* and "collector efficiency" and exhibits an intermediate value for "solar fraction". In the following, we will investigate if the solution is unique and how the combination between different objectives will impact the configuration.

3.3.1. Objective plots

Fig. 8, (a) to (f), present the evolution of the "solar fraction" as function of different parameter combinations. Fig. 8 (a) and (b) show "solar fraction" as function of V_s and S_{col} for $\min(\Delta T_{col})$, $\min(V_{lim}/V_{ws})$, $\min(V_{ws})$ and $\max(V_{ws})$, respectively. Both figures are very similar and exhibit a clear dependency to V_s and S_{col}. Indeed, for increasing S_{col} and V_s, "solar fraction" increases up to a plateau whose values are much important for $\max(V_{ws})$. The influence from $\min(V_{ws})$ to $\max(V_{ws})$ is so a positive shift of the values of "solar fraction". Moreover, optima could be deduced from these figures by investigating the inflection line before the plateau.

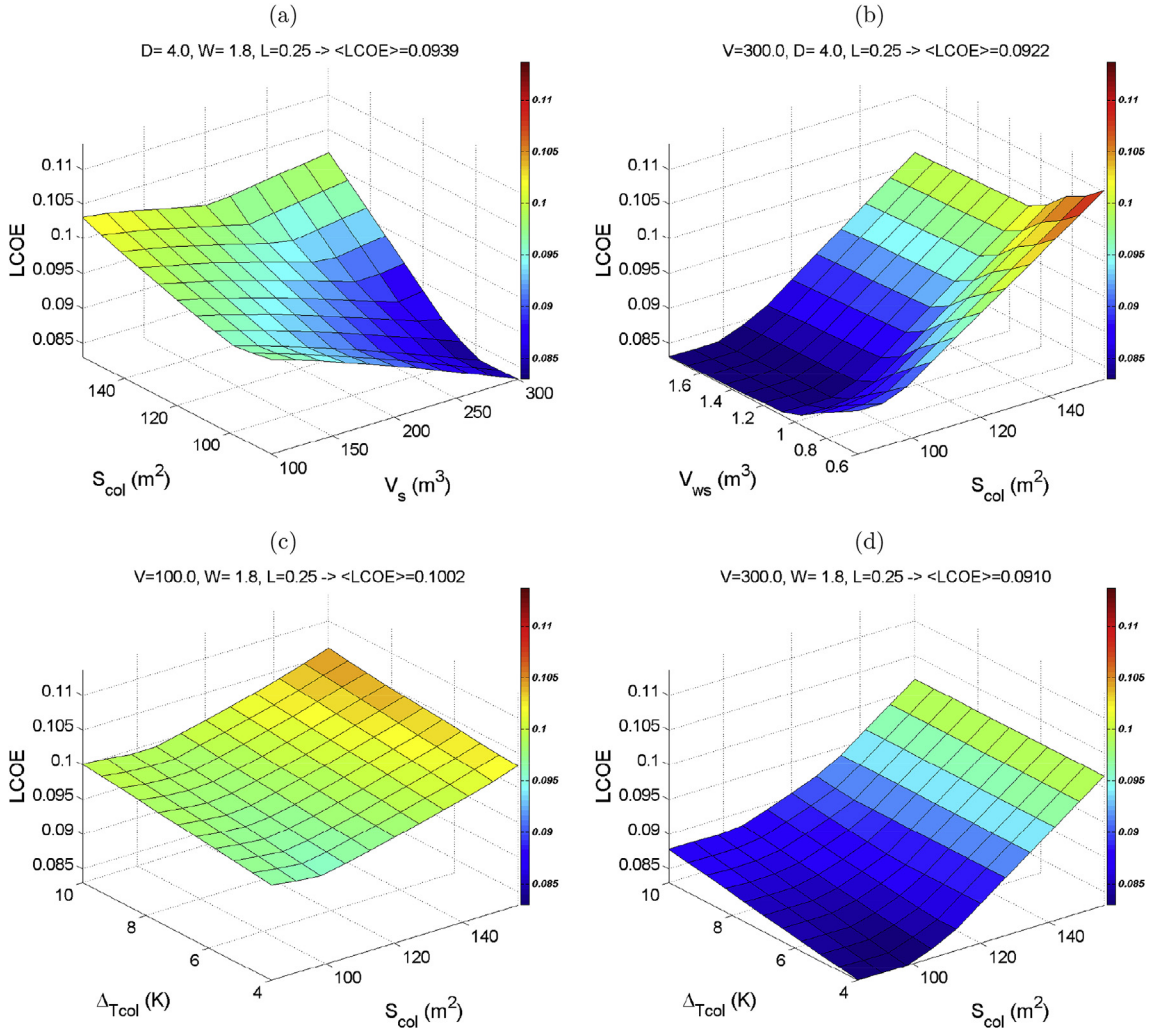

Fig. 9. *LCOE* as function of the different parameters. The information given on the top of each plots corresponds to the values of the parameters keeping constant and to the ensemble average $\langle \cdot \rangle$ of the criterion for the corresponding plot.

Fig. 8 (c) and (d) illustrate "solar fraction" as function of V_{ws} and V_s for $\min(\Delta T_{col})$, $\min(V_{lim}/V_{ws})$, $\min(S_{col})$ and $\max(S_{col})$, respectively. For $\min(S_{col})$, the influence of V_{ws} and V_s is almost bi-linear with an inflection line at $V_{ws} \sim 1m^3$. This indicates that the volume of DHW should insure the daily needs in minimum, and to be efficient V_{ws} should be in capacity to a storage superior to one day. We can note also the presence of the plateau when S_{col} is maximum in Fig. 8 (d). "solar fraction" is almost also bi-linear with S_{col} and ΔT_{col} for $\min(V_s)$ with stronger values for low values of ΔT_{col} (Fig. 8 (e)). However when V_s is maximum, the influence of ΔT_{col} is weak (Fig. 8 (f)) which means that V_s should reach a critical value where the influence of ΔT_{col} is weak. In any case ΔT_{col} has to be minimum to obtain maximum values of "solar fraction".

Fig. 9, (a) to (d), present the results on *LCOE* as function of different parameter combinations. Fig. 9 (a) shows a bowl in *LCOE* as function of V_s and S_{col} for $\min(\Delta T_{col})$, $\min(V_{lim}/V_{ws})$ and $\max(V_{ws})$ (a). Indeed, the minimum of *LCOE* is obtained here for $\min(S_{col})$ and $\max(V_s)$ and the global tendency is a decreasing *LCOE* for an increase V_s and a decrease S_{col}. The configuration for the minimum of *LCOE* ($\min(S_{col})$ and $\max(V_s)$) is in adequation as the one obtained in Ref. [21] for Barcelona which has also a Mediterranean climate.

In Fig. 9 (b), $V_{ws} \sim 1m^3$ defines an inflection line and the minimum values of *LCOE* are obtained only when $V_{ws} \geq 1.2m^3$. This confirms the explanation given for "solar fraction". Indeed if the DHW have a storage volume less than one day, two consecutive days of bad sunshine will involve the use of supply energy to insure the hot water needs, thus generating extra costs.

In one hand, the influence of ΔT_{col} seems to be weak in Fig. 9 (c) and (d) since the slope in its direction is not pronounced for $\min(V_s)$. In another hand, the slope in S_{col}-direction is significant for $\max(V_s)$ which is also representative to a strong correlation for *LCOE* between S_{col} and V_s.

Fig. 10 (a), (b), (c) and (d) shows almost the opposite behavior for "collector efficiency" in comparison of Fig. 9. The influence of V_s is more important for "collector efficiency" since the slope in V_s-direction is more pronounced (Fig. 10 (a)). Tendencies on Fig. 10 (c) and (d) confirm the low sensitivity of the solar collector efficiency to ΔT_{col} (Fig. 7). The other configurations for all the objective criteria (not shown here) do not demonstrate an influence of V_{lim}/V_{ws}.

These results are complementary to the ones obtained from the sensitivity study. Indeed, the sensitivity study makes possible to identify the most influential parameters on the criteria to be optimized and gives the tendencies of the influence of the different parameters. The results of this section, targeted on the most influential parameters, enables to refine the analysis. They are no

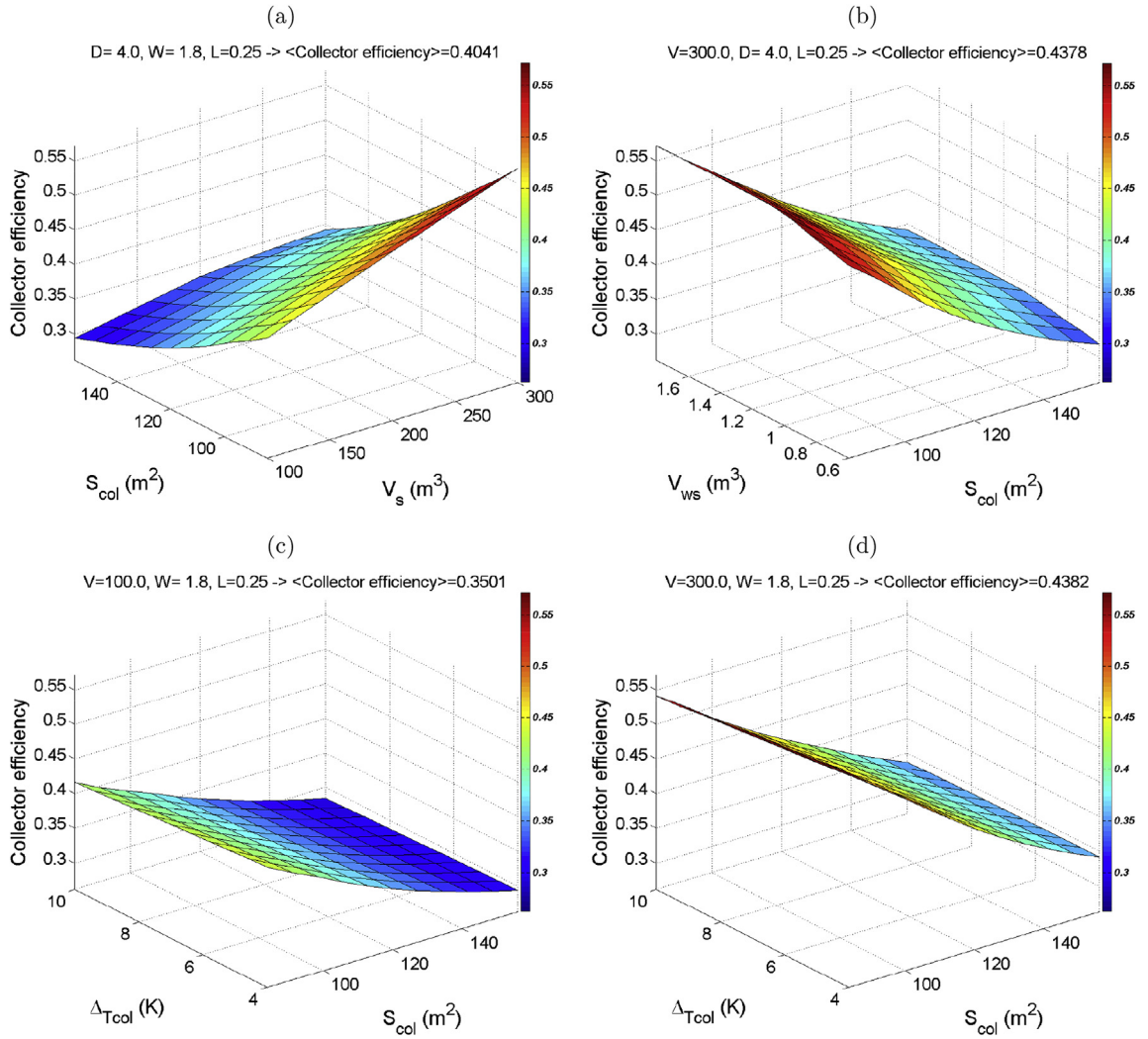

Fig. 10. Collector efficiency as function of the different parameters. The information given on the top of each plots corresponds to the values of the parameters keeping constant and to the ensemble average $\langle \cdot \rangle$ of the criterion for the corresponding plot.

longer limited on the minimum and maximum values of the study range of the parameters, but also for intermediate values. This representation is useful to refine the choices with respect to a certain number of constraints. For our study, the volume of DHW should be superior to one day need in order to avoid the use of supply energy. Moreover, the choice of solar collectors surface is correlated to inter-seasonal storage volume to obtain the best "solar fraction" and "collector efficiency" while *LCOE* decreases for larger V_s and smaller S_{col}.

3.3.2. Objective combinations

If the analysis of the systems can be done independently on various optimization criteria, the choices to be made in the final decision rely more and more on a combination of the criteria, with a weighting that depends on the sensitivities of the final decision-makers. In this section, the different objective criteria combinations are so presented.

Fig. 11 shows the two objectives "solar fraction" and "collector efficiency" colored by *LCOE* (a), S_{col} (b), V_s (c) and V_{ws} (d). For each graph, each colored point in the 2D plots corresponds to one simulation in order to magnify the possible correlations between the different output objectives. The optimized system needs to maximize "Solar fraction" and "Collector efficiency", and to minimize *LCOE*. To reach this latter condition, the area of interest shown in Fig. 11 (a), is delimited in the range $[0.9, 1]$ for "solar fraction" and $[0.4, 0.56]$ for "collector efficiency" which corresponds to low values of *LCOE* ($< 0.1€/kWh$). Moreover, the correlation between *LCOE* and "collector efficiency" is confirmed. Indeed, *LCOE* decreases for increasing "collector efficiency" by following transverse lines. We can note also that maximum values of "collector efficiency" is obtained for minimum values of *LCOE*. Fig. 11 (b) investigates the dependency of the two objectives due to the surface collectors S_{col}. For a given S_{col} surface, the "solar fraction" varies very substantially, which confirms the results of the sensitivity section, and this variation is more significant when the collector surface is small. In fact, The different transverse lines correspond to one value of S_{col} therefore we can almost find the maximum value of "solar fraction" for a given S_{col}. Based in the area of interest deduced of analysis on

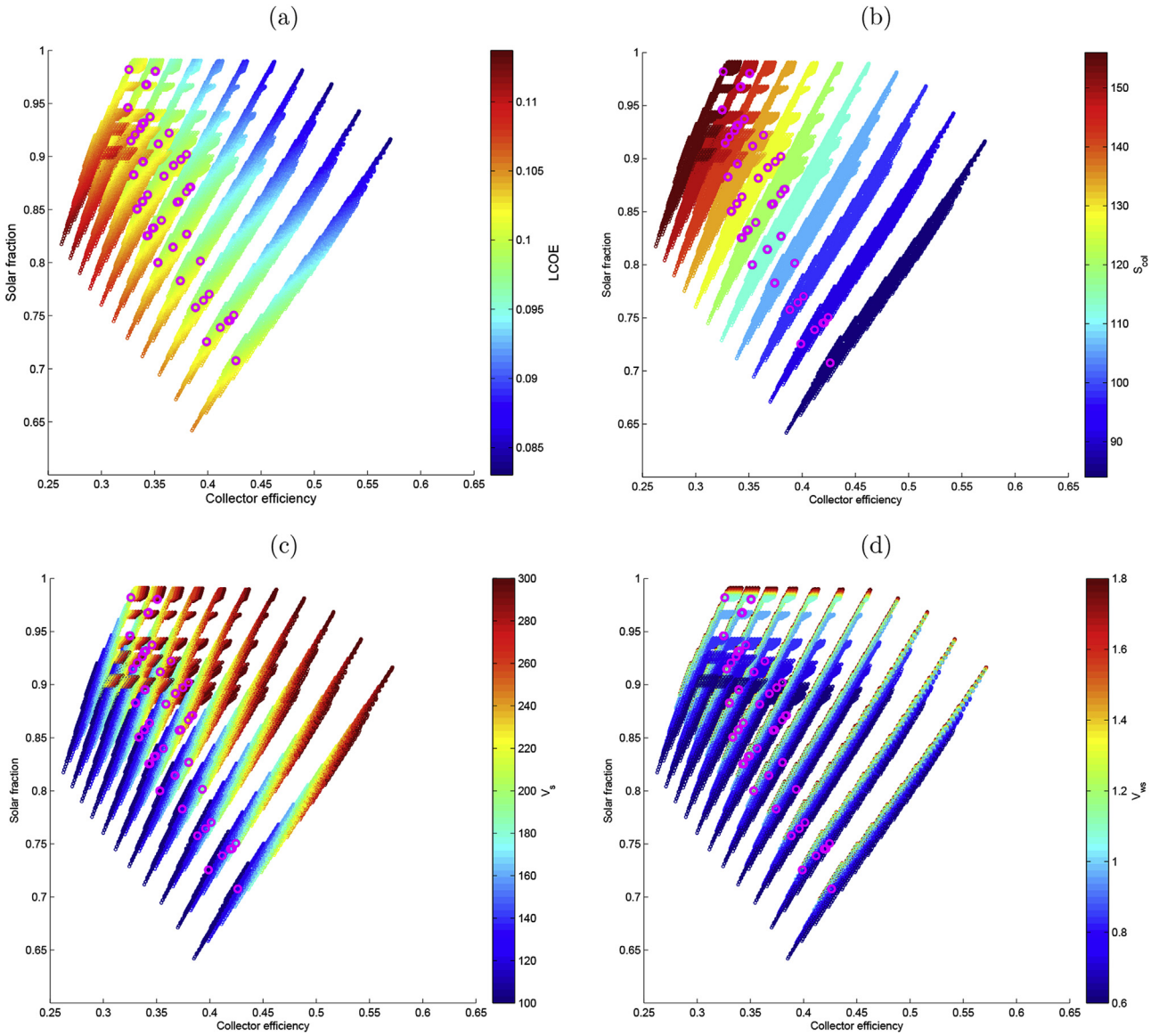

Fig. 11. Solar fraction and collector efficiency objectives colored by *LCOE*, S_{col}, V_s and V_{ws}. Each point in the 2D plots corresponds to one of 161051 simulations. Magenta circles correspond to the simulations giving $|LCOE - 0.1| \leq 10^{-5}$.

Fig. 11 (a), $S_{col} < 125m^2$ should be favored.

Fig. 11 (c) demonstrates that a large value of V_s is needed to reach the objective zone and the dependency of V_s is clearly shown, that is to say, "collector efficiency" is getting better for increasing V_s. Finally, there is no clear behavior for V_{ws} in Fig. 11 (d) since all the solutions are represented everywhere, however the maximum values of "solar fraction" is obtained for maximum value of V_{ws}. The explanation is that a large V_{ws} enables to constitute a larger storage for DHW and it allows to get independent of several days of bad weather. The figures for two objectives colored by ΔT_{col} and V_{lim}/V_{ws} do not give additional information since the points are distributed over the whole range of the objectives.

To summarize the area of interest, which is the zone of maximum "solar fraction", maximum "collector efficiency" and minimum *LCOE*, corresponds to minimum S_{col}, maximum V_s, and V_{ws} superior to $1.2m^3$. The analysis is no longer evident, if we start weighing the criteria for final selection. This means that to privilege the minimization of auxiliary energy and the minimization of costs could be antagonistic. For this purpose, based on the Pareto solutions calculated via a weighted-sum method [21,39], which combines two different objectives (f_1 and f_2) using a linear weighted-sum (*WS*):

$$max(WS) = (1-\lambda)f_1^*(x) + \lambda f_2^*(x) \tag{29}$$

where x denotes the variables of the model, λ is the positive weight, $f_1^*(x)$ and $f_2^*(x)$ are the normalized objectives:

$$f_i^*(x) = \frac{f_i(x) - min(f_i(x))}{|max(f_i(x)) - min(f_i(x))|} \text{ if the objective is to maximize} \tag{30}$$

$$f_i^*(x) = \frac{max(f_i(x)) - f_i(x)}{|max(f_i(x)) - min(f_i(x))|} \text{ if the objective is to minimize} \tag{31}$$

where $i = 1, 2$. In other words, the input parameters (S_{col}, V_s, V_ws, ΔT_{col}, V_{lim}/V_{ws}) of the simulations corresponding to $max(WS)$ are quantified for increasing λ.

Fig. 12 shows the results of weighted-sum method for "collector efficiency" and *LCOE*. The best configurations for these two objectives are almost always obtained for $\max(V_s)$, for $\min(S_{col})$ and for $\max(V_{ws})$. There is a weak influence of V_{lim}/V_{ws} when "collector efficiency" has no weight ($\lambda = 1$). The value of this parameter, which indicates the position of the thermocline to trigger the storage DWH, is then constant to the maximum value of V_{lim}/V_{ws}. These results demonstrates that the objective criteria "collector efficiency" and *LCOE* give almost the same information and the small differences occur when the weight of *LCOE* is important.

Fig. 13 exhibits the results of weighted-sum method for "collector efficiency" and "solar fraction". When "solar fraction" is more

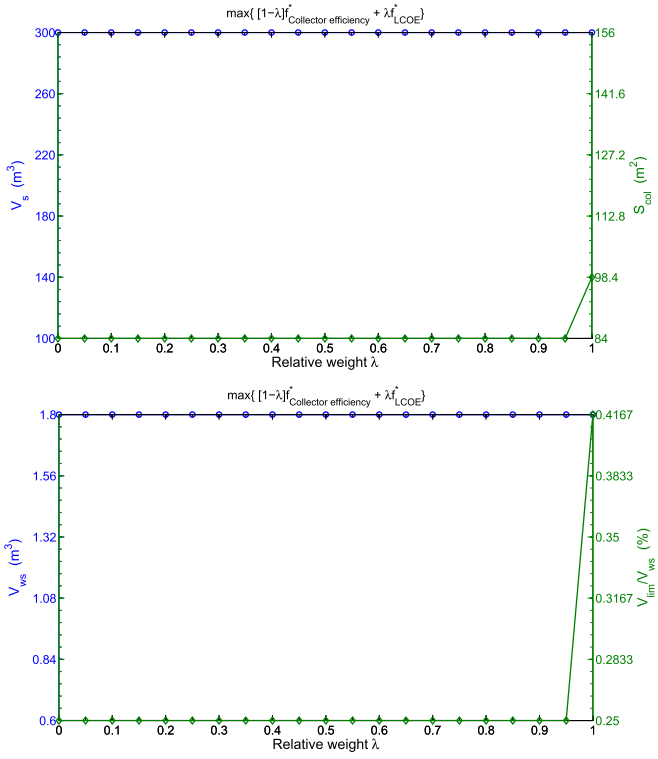

Fig. 12. Weighted-sum method for "collector efficiency" and *LCOE*.

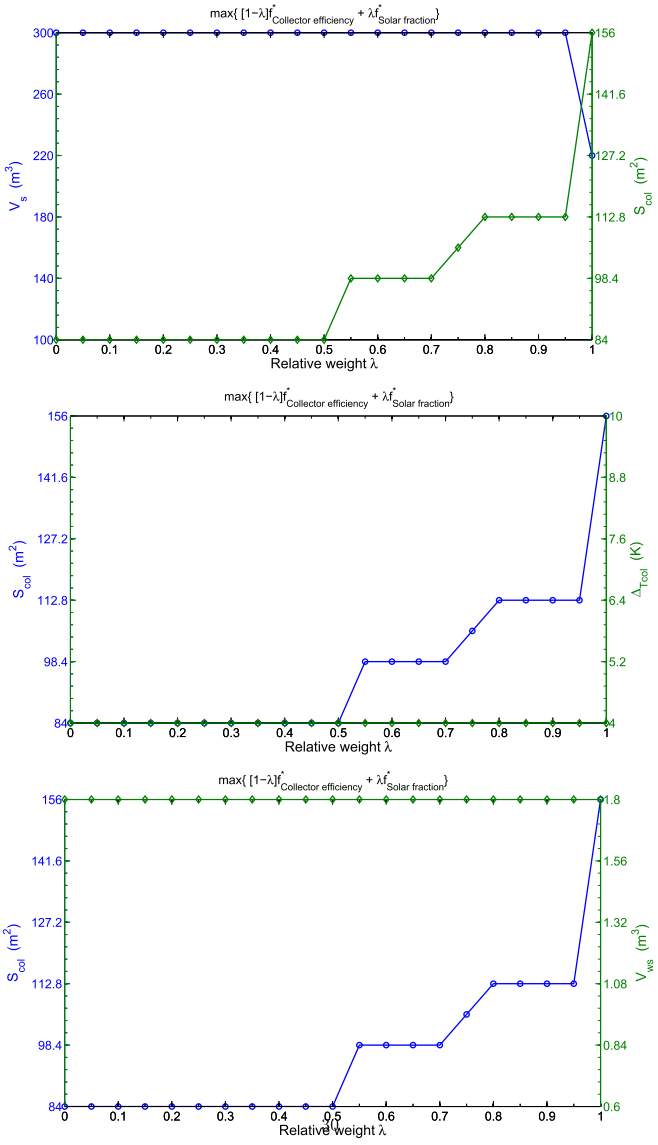

Fig. 13. Weighted-sum method for "collector efficiency" and "solar fraction".

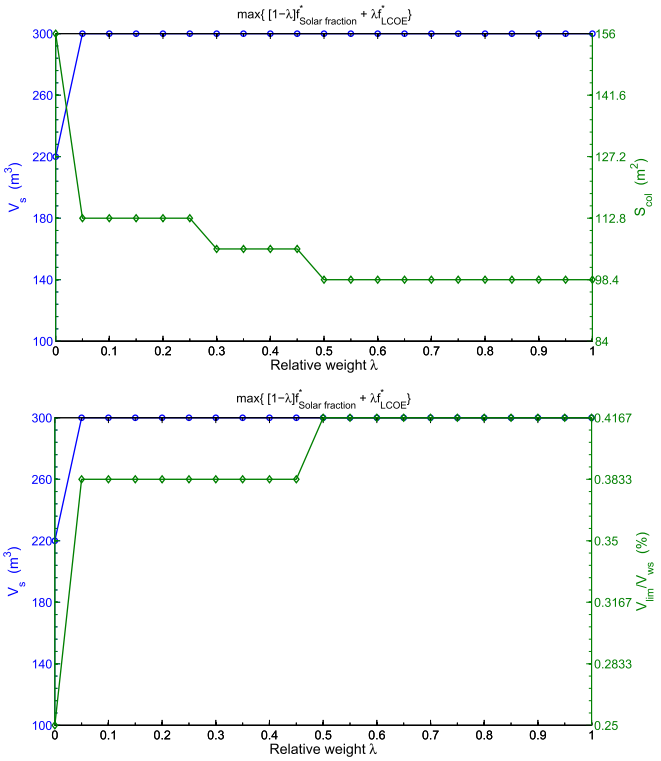

Fig. 14. Weighted-sum method for "solar fraction" and *LCOE*.

important ($\lambda > 0.5$), on the one hand the impact of S_{col} is increasingly stronger and its value changes from $\min(S_{col})$ to $\max(S_{col})$. On the other hand, V_s acts weakly only when there is no weight of "collector efficiency". ΔT_{col} and V_{ws} has to be chosen constant to its minimum and maximum value to obtain the best configurations, respectively. This shows, as expected, that the most important parameters when "collector efficiency" and "solar fraction" are combined, is S_{col} while the other parameters are of less impact. In other words, the best compromise is here obtained by varying the solar collectors surface S_{col}.

Fig. 14 shows the results of weighted-sum method for "solar fraction" and *LCOE*. Fig. 14 (top) is almost the mirror of Fig. 13, as expected since "collector efficiency" is correlated with *LCOE*. Differences can be noted for S_{col}. Indeed the minimum of S_{col} is not reached for small "solar fraction" weights. The objective criteria "solar fraction" and *LCOE* follow the same dynamics concerning V_s and V_{lim}/V_{ws}. "Solar fraction" is dominant for one intermediate value of V_s and the minimum value of V_{lim}/V_{ws}. For increasing weight of *LCOE*, V_s is maximum and V_{lim}/V_{ws} presents a plateau at $V_{lim}/V_{ws} \sim 0.38$. The other configurations do not give additional information. As a consequence, in presence of a large inter-seasonal storage volume, to vary solar collectors surface is the main parameter in order to get a good "solar fraction" and small *LCOE*. The choice of these parameters can also be deduced from the combination between "collector efficiency" and "solar fraction".

4. Conclusion

In the present work, we propose an analysis strategy for multi-criteria optimization applied to inter-seasonal solar heat storage for residential building energy needs. The inter-seasonal solar system includes two thermal storages, in the short and long term, to ensure the needs for Domestic Hot Water (DHW) and for heating. Particular attention is being conducted on the control and prioritization parameters of energy fluxes. The energy monthly dynamics of the system indicates that extra energy is needed during the months of January and February to cover heating demand. In addition extra-energy is also necessary, at various periods along the year, to cover DHW demand if the weather is very little sunny during for more than two days.

The sensitivity analysis that has been applied enables to quantify the influence of the different parameters and their interactions for three output objectives. For studied system, the increase of the collector surface, S_{col}, the volumes of inter-season storage V_s and of DHW V_{ws} play very favorably for the increase of the solar fraction. However, this increase is partially attenuated by the coupling effect between V_s and S_{col}.

Based on the sensitivity analysis, several simulations are performed by using a regular discretization of five parameters in order to investigate multi-objective optimization. This enables to refine the choices with respect to a certain number of constraints. The development of inter-seasonal solar heat storage corresponds to the region of maximum "solar fraction", maximum "collector efficiency" and minimum *LCOE*. In the range of parameter variation, the area of interest corresponds to minimum S_{col}, maximum V_s, and V_{ws} superior to $1.2m^3$. If the analysis of the systems can be done independently on various optimization criteria, the final decision on the system selection relies more and more on a combination of criteria, with a weighting that depends on the sensitivities of the final decision-makers. For this purpose, Pareto solutions calculated via a weighted-sum method, which combines two different objectives using a linear weighted-sum (WS), are implemented. Future works will be extended to hybrid and multi-source energetic systems by applying the same strategy.

Acknowledgment

The authors would like to acknowledge the financial support provided by CONICYT / FONDAP 15110019 "Solar Energy Research Centre" SERC-Chile, Fondecyt Postdoctoral grant n°3140014, FIC-R 30137092 funded by Atacama Government and the Education Ministry of Chile Grant PMI ANT 1201. The authors thank Y. Jobic for the computer support. They are also thankful to A. Girard, E. Fuentealba, and L. Tadrist for fruitful discussions.

References

[1] Lund P. Optimization of a community solar heating system with a heat pump and seasonal storage. Sol Energy 1984;33:353–61.
[2] Jan-Olof Dalenbäck (CIT Energy Management AB). Success factors in solar district heating (SDH), WP2 - micro analyses report. Dec. 2010. Technical Report.
[3] Sørensen (PlanEnergi) A. Solar district heating guidelines, collection of fact sheets WP3 - D3.1 & D3.2. Aug. 2012. Technical Report.
[4] Gao L, Zhao J, Tang Z. A review on borehole seasonal solar thermal energy storage. Energy Procedia 2015;70:209–18.
[5] Novo AV, Bayon JR, Castro-Fresno D, Rodriguez-Hernandez J. Review of seasonal heat storage in large basins: water tanks and gravelwater pits. Appl Energy 2010;87:390–7.
[6] Schmidt T, Mangold D, Mller-Steinhagen H. Central solar heating plants with seasonal storage in Germany. Sol Energy 2004;76:165–74. Solar World Congress 2001.
[7] Oliveti G, Arcuri N, Ruffolo S. First experimental results from a prototype plant for the interseasonal storage of solar energy for the winter heating of buildings. Sol Energy 1998;62:281–90.
[8] Oliveti G, Arcuri N, Ruffolo S. Effect of climatic variability on the performance of solar plants with interseasonal storage. Renew Energy 2000;19:235–41.
[9] Ucar A, Inalli M. Thermal and economical analysis of a central solar heating system with underground seasonal storage in Turkey. Renew Energy 2005;30:1005–19.
[10] Ucar A, Inalli M. Thermal and economic comparisons of solar heating systems with seasonal storage used in building heating. Renew Energy 2008;33:2532–9.
[11] Ampatzi E, Knight I, Wiltshire R. The potential contribution of solar thermal collection and storage systems to meeting the energy requirements of north

european housing. Sol Energy 2013;91:402–21.
[12] Franke R. Modeling and optimal design of a central solar heating plant with heat storage. In: The ground using Modelica. Espoo, Finland; 2014.
[13] Pinel P, Cruickshank CA, Beausoleil-Morrison I, Wills A. A review of available methods for seasonal storage of solar thermal energy in residential applications. Renew Sustain Energy Rev 2011;15:3341–59.
[14] Lanini S, Delaleux F, Py X, Olivs R, Nguyen D. Improvement of borehole thermal energy storage design based on experimental and modelling results. Energy Build 2014;77:393–400.
[15] Lhendup T, Aye L, Fuller RJ. In-situ measurement of borehole thermal properties in melbourne. Appl Therm Eng 2014;73:287–95.
[16] Claesson J, Hellstrm G. Multipole method to calculate borehole thermal resistances in a borehole heat exchanger. HVAC R Res 2011;17:895–911.
[17] Atam E, Helsen L. Ground-coupled heat pumps: Part 2 - literature review and research challenges in optimal design. Renew Sustain Energy Rev 2016;54:1668–84.
[18] Muñoz-Criollo JJ, Cleall PJ, Rees SW. Factors influencing collection performance of near surface interseasonal ground energy collection and storage systems, Geomechanics for Energy and the Environment 6. 2016. p. 45–57. Themed Issue on Selected Papers Symposium of Energy Geotechnics 2015 Part I.
[19] Doughty C, Hellstrom G, Tsang CF, Claesson J. A dimensionless parameter approach to the thermal behavior of an aquifer thermal energy storage system. Water Resour Res 1982;18:571–87.
[20] Kroll J, Ziegler F. The use of ground heat storages and evacuated tube solar collectors for meeting the annual heating demand of family-sized houses. Sol Energy 2011;85:2611–21.
[21] Tulus V, Boer D, Cabeza LF, Jimnez L, Guilln-Goslbez G. Enhanced thermal energy supply via central solar heating plants with seasonal storage: a multi-objective optimization approach. Appl Energy 2016;181:549–61.
[22] Kim J, Hong T, Jeong J, Koo C, Jeong K. An optimization model for selecting the optimal green systems by considering the thermal comfort and energy consumption. Appl Energy 2016;169:682–95.
[23] Delgarm N, Sajadi B, Delgarm S. Multi-objective optimization of building energy performance and indoor thermal comfort: a new method using artificial bee colony (abc). Energy Build 2016;131:42–53.
[24] Bonnin M, Azzaro-Pantel C, Domenech S, Villeneuve J. Multicriteria optimization of copper scrap management strategy. Resour Conserv Recycl 2015;99:48–62.
[25] Penna P, Prada A, Cappelletti F, Gasparella A. Multi-objectives optimization of energy efficiency measures in existing buildings. Energy Build 2015;95:57–69 [Special Issue: Historic, historical and existing buildings: designing the retrofit. An overview from energy performances to indoor air quality].
[26] Renaldi R, Kiprakis A, Friedrich D. An optimisation framework for thermal energy storage integration in a residential heat pump heating system. Appl Energy 2017;186(Part 3):520–9 [Sustainable Thermal Energy Management (SusTEM2015)].
[27] Hottel HC, Willier A. Evaluation of flat-plate solar collector performance. In: Trans. of the Conf. on the Use of Solar Energy. The Scientific Basis, Vol. II, Part 1, Section A. University of Arizona Press; 1958. p. 74–104.
[28] Florschuetz L. Extension of the hottel-whillier model to the analysis of combined photovoltaic/thermal flat plate collectors. Sol Energy 1979;22:361–6.
[29] Duffie JA, Beckman WA. Solar engineering of thermal processes. fourth ed. John Wiley & Sons; 2013.
[30] Hadorn JC. Thermal energy storage for solar and low energy buildings - state of the art, International Energy Agency Solar Heating & Cooling Programme. Edicions de la Universitat de Lleida; 2005.
[31] Hasnain S. Review on sustainable thermal energy storage technologies, part i: heat storage materials and techniques. Energy Convers Manag 1998;39:1127–38.
[32] Segond G. Etudes des couplages thermohydrauliques en régime variable d'un système thermique avec stockage : application à la production d'eau chaude sanitaire à partir de la valorisation d'une source de chaleur basse température (Studies of thermohydraulic couplings in variable regime of a thermal system with storage: application to the production of domestic hot water from the valuation of a low temperature heat source). Ph.D. thesis; 2015. URL: http://www.theses.fr/2015AIXM4722.
[33] Xu J, Wang R, Li Y. A review of available technologies for seasonal thermal energy storage. Sol Energy 2014;103:610–38.
[34] Consortium OSM. Openmodelica. 2016. https://openmodelica.org.
[35] Jenni-Energietechnik. Building-solar. 2007. http://jenni.ch/jenni-mehrfamilienhaus.html.
[36] Hamby DM. A review of techniques for parameter sensitivity analysis of environmental models. Environ Monit Assess 1994;32:135–54.
[37] Iooss B, Lemaître P. A review on global sensitivity analysis methods. Boston, MA: Springer US; 2015. p. 101–22.
[38] Montgomery D. Design and analysis of experiments. eighth ed. John Wiley & Sons; 2013.
[39] Ehrgott M. Multicriteria optimization. Springer-Verlag Berlin Heidelberg; 2005.